The University of Sydney

Department of Civil Engineering
Sydney NSW 2006
AUSTRALIA

http://www.civil.usyd.edu.au/

Centre for Advanced Structural Engineering

Elastic and Plastic Effective Width Equations for Unstiffened Elements

Research Report No R819

Bambach M.R. BE
Rasmussen K.J.R. MScEng, PhD

May 2002

The University of Sydney

Department of Civil Engineering
Centre for Advanced Structural Engineering
http://www.civil.usyd.edu.au/

Elastic and Plastic Effective Width Equations for Unstiffened Elements

Research Report No R819

Bambach M.R. BE
Rasmussen K.J.R. MScEng, PhD

May 2002

Abstract:

Current American design provisions treat unstiffened elements under stress gradients as if they were uniformly compressed for effective width calculations. Australian, British and European design provisions allow accurate calculation of the elastic buckling coefficient, however the same effective width equation for compressed elements is used for elements with stress gradients. In all cases, the design provisions produce conservative bending capacities for sections containing unstiffened elements under stress gradients. This report presents a design method for calculating the effective width of these elements, based on plate test results of unstiffened elements under strain gradients varying from pure compression to pure bending. It is shown that both elastic and plastic effective widths may be derived from the test results, and effective width methods based on both principles may be used for design.

Keywords:

Unstiffened elements, stress gradient, elastic effective width, plastic effective width, plate tests, design

Copyright Notice

Department of Civil Engineering, Research Report R819
Elastic and Plastic Effective Width Equations for Unstiffened Elements

mbambach@civil.usyd.edu.au

Published by:
Department of Civil Engineering
The University of Sydney
Sydney NSW 2006
AUSTRALIA

May 2002

http://www.civil.usyd.edu.au

INTRODUCTION

Open thin-walled sections usually consist of stiffened and unstiffened component plates. If these elements are sufficiently slender, the section will locally buckle at a load less than the ultimate load carrying capacity. The section will continue to resist load after local buckling due to the redistribution of longitudinal stress from the most flexible regions. This redistribution may be simplified for design purposes by assuming that certain regions of the cross-section remain effective up to the yield point of the material, whilst the remainder is ineffective in resisting load. The effective width method is a universal tool, as it may be applied to any section geometry. Current specifications for the design of open thin-walled sections provide equations for determining the effective width of stiffened and unstiffened elements, and the ultimate capacity of the section is calculated from the effective section properties. However, for cross-sections in bending with unstiffened elements under stress gradients, current design provisions have been shown to be unduly conservative (Chick and Rasmussen 1999).

Extensive experimental and analytical studies on stiffened elements (supported along both longitudinal edges) have been carried out and have led to well-established equations for the estimation of the effective width of such elements in uniform compression and under stress gradients. In comparison, experimental investigations on unstiffened elements (supported along one longitudinal edge) are quite limited. In the 1970s the applicability of the effective width concept to unstiffened elements under uniform compression was studied in detail by Kalyanaraman et al. (1977), who tested a large number of beams and short columns that contained web elements that were fully effective. Tests of a similar nature previously reported by Winter (1947, 1970) and the experimental and analytical research by Kalyanaraman et al. (1977), led to the adoption of the effective width approach for uniformly compressed unstiffened elements in the 1986 edition of the AISI Specification.

Beam tests on sections that contain fully effective webs and simple edge stiffeners subjected to stress gradients have been reported by Desmond et al. (1981) and Winter (1947), and on open channels with inclined flanges under stress gradients by Rhodes (2000). Single plate test data for unstiffened elements with stress gradients have only been reported by Rhodes et al. (1975), where results of 4 tests on individual plates simply supported on three sides are given for varying values of load eccentricity. Due to the lack of test data, the AISI (1996) treats unstiffened elements with stress gradients as if they were uniformly compressed for effective width calculations. The Australian, British and European codes allow accurate calculation of the elastic buckling coefficient, however the same effective width equation for compressed elements is used for elements with stress gradients. In all cases, the design provisions produce bending capacities up to 50% conservative for sections containing unstiffened elements under stress gradients (Chick and Rasmussen 1999).

In a companion report (Bambach and Rasmussen 2002b), the results of 80 plate tests of unstiffened plate elements, under strain gradients varying from pure compression to pure bending are presented. This report presents strength curves derived from the plate tests, where the effective width is assumed to be under both elastic (linear) and plastic (constant yield) stress distributions. Design equations are presented for calculating both elastic and plastic effective widths.

PLASTIC STRAINS IN SECTIONS

In order that a coherent design solution may be obtained from the test results, one must first examine the strain condition that exists in structural sections at ultimate. For sections where the unstiffened element is in pure compression, such as compression members and I-sections and channel sections in major axis bending, there is no difference to the design philosophy if the ultimate strain is at the yield strain or at two times the

yield strain for example, as far as the flange is concerned, since as the unstiffened element is assumed to be at the yield stress in both situations, an effective width at the yield stress is applicable. When we consider an I-section in minor axis bending however, if the maximum strain in the section at ultimate is the yield strain, an effective width with a stress gradient varying from the yield stress to zero stress would be appropriate (hereafter termed an elastic effective width). If the strain gradient, or curvature, was infinitely large (fully plastic section), an effective width with a stress gradient of constant yield stress would be appropriate (hereafter termed a plastic effective width). For most practical sections one would expect a strain condition at ultimate somewhere between these two conditions.

Experimental studies by Chick and Rasmussen (1999) and Rusch and Lindner (2001) on I-sections in minor axis bending, and Beale et al. (2001), Rhodes (2000), and Yiu and Pekoz (2001) on plain channel sections in minor axis bending, have shown that these sections often exhibit post-elastic behavior. For example an I-section in minor axis bending with flange slenderness 1.0 (Equation 1) tested by Chick (1997) reached a curvature of 2.1 times the yield curvature at ultimate, and a similar section with flange slenderness of 1.44 tested by Rusch and Lindner (2001) reached a curvature of approximately 3 times the yield curvature. Experiments on plain channels and channels with inclined flanges in minor axis bending (producing compression at the flange tip) by Rhodes (2000) showed full plastic capacity for b/t ratios less than 15, and post-elastic capacity up to approximately 30. A similar result was found by Beale et al. (2001) from tests on plain channels in minor axis bending. Yiu and Pekoz (2001) proposed that plain channels in minor axis bending (producing compression at the flange tip) exhibit post-elastic capacity for flange slenderness ratios less than 0.859.

$$l = \sqrt{\frac{f_y}{f_{cr}}} \tag{1}$$

$$f_{cr} = \frac{kp^2 E}{12(1-u^2)\left(\frac{b}{t}\right)^2} \tag{2}$$

COMPARISON OF ELASTIC AND PLASTIC EFFECTIVE WIDTHS

The use of elastic effective widths adjacent to the supported edge, or plastic effective widths at an eccentricity to the supported edge, is central to the design philosophy and to the ensuing design equations for unstiffened elements under strain gradients. For the load case of compressive strain at the free edge and zero strain at the supported edge, the elastic effective width is calculated by equating the ultimate axial force on the element in the test to a stress block that varies linearly from yield at the unsupported edge of the effective width to zero at the supported edge of the element (Figure 1). The plastic effective width is calculated by equating the same ultimate axial force on the element in the test to a stress block of constant yield stress on the effective width (Figure 2). For this load case, elastic effective widths will be of the order of two times the magnitude of those assuming plastic effective widths.

Calculations have shown that for the strain gradients tested, both elastic and plastic effective widths satisfy the ultimate axial force on the element in the test (with the exception of the load case of compressive strain at the supported edge and zero strain at the free edge, where the ultimate axial force is slightly underestimated by the elastic effective width equations for less slender elements). The plastic effective width is positioned at an eccentricity to the supported edge, such that the moment of the yield block (about the supported edge) is equal to the moment of the force and moment stress blocks at ultimate in the tests (about the supported edge). The elastic effective width, congruent with current design standards, is positioned adjacent to the supported edge, and the linear stress block has a fixed eccentricity of 2/3rds of the

elastic effective width. The plastic effective width method is thus a two degree of freedom solution (effective width and eccentricity), while the elastic method is a one degree of freedom solution (effective width). Calculations have shown that the elastic effective width method underestimates the ultimate moment in the tests.

It is shown in a companion report (Bambach and Rasmussen 2002a), that good agreement with tests on structural sections, including I-sections and channel sections in minor axis bending, can be achieved by using inelastic stress distributions. For unstiffened elements in bending, these stress distributions involve constant (plastic) stress blocks at yield on the effective widths. The proposed inelastic design calculation is consistent with the design procedure for cross-sections containing stiffened compression elements described in Sections 3.3.2.3 and C3.1.1(b) of AS/NZS4600 (1996) and the AISI Specification (1996) respectively. It is also consistent with the experimental observation discussed in the previous section that cross-sections containing unstiffened elements under strain gradients often have ultimate compressive strains exceeding the yield strain in their ultimate limit state. Plastic effective widths, therefore, satisfy exactly the ultimate force and moment values from the plate tests, and are congruent with the proposed inelastic design model for structural sections.

As mentioned previously, elastic effective widths are congruent with current design standards, however the moment capacity in the plate tests is underestimated. It is shown in the companion report (Bambach and Rasmussen 2002a) that while elastic effective widths underestimate the moment capacity of the plate tests, good agreement with tests on structural sections can be achieved with the inelastic model. Since both elastic and plastic effective width methods are applicable, elastic and plastic effective widths are derived from the plate tests and are presented in this report.

PLASTIC EFFECTIVE WIDTH AND ECCENTRICITY RESULTS

The plastic effective widths and eccentricities are calculated from the stress values of the applied compressive axial force (N) and bending moment (M) at the ultimate condition in the tests. The values of equivalent uniform stress (f_{Cult}) and bending stress (f_{Mult}) derived from the ultimate force and moment are presented in Bambach and Rasmussen (2002b), as are the values of strain at the ultimate condition. The applied force and moment stress blocks are equilibrated to an effective width at full yield (Figure 2). The effective width is calculated such that the net forces are equal, and the eccentricity is calculated such that the moments of the stress blocks about the supported edge are equal. For the load case shown in Figure 2, the equations for the plastic effective width (b_e) and eccentricity of the resultant force of the yield stress block from the supported edge (ecc) are given by Equations 3,4.

$$\frac{b_e}{b} = \frac{f_{Cult}}{f_y} = \frac{\frac{N}{bt}}{f_y} \tag{3}$$

$$\frac{ecc}{b} = \frac{b\left[\frac{f_{Cult}}{2} + \frac{f_{Mult}}{6}\right]}{f_y b_e} = \frac{b\left[\frac{N}{2bt} + \frac{M}{b^2 t}\right]}{f_y b_e} \tag{4}$$

Equation 3 for the plastic effective width is used for all load cases tested. Equation 4 for the eccentricity will differ depending on the load case being analysed, however for all load cases the principle of equating the moment of the ultimate stress blocks about the supported edge is used. The eccentricity of the effective width from the supported and unsupported edges, designated eccentricity1 ($ecc1$) and eccentricity2 ($ecc2$) respectively in Figure 2, may be deduced from the eccentricity of the force and the effective width. For

strain gradients where tension exists in the element, the plastic effective width factor (b_e/b) gives the effective width of the *compressed portion* of the element.

ELASTIC EFFECTIVE WIDTH RESULTS

The elastic effective widths are calculated from the applied compressive axial force (N) at the ultimate condition in the tests. The applied force stress block (f_{Cult}) is equilibrated to an effective width with a linearly varying stress distribution (Figure 1). For the load case shown in Figure 1, the equation for the elastic effective width is given by Equation 5. For strain gradients where tension exists in the element, the elastic effective width factor (r) gives the total effective width of the element, measured from the supported edge, and is thus congruent with the effective width factor (r) currently used in international design standards.

$$r = 2\left(\frac{f_{Cult}}{f_y}\right) = 2\left(\frac{N}{\frac{bt}{f_y}}\right) \tag{5}$$

STRENGTH CURVES

Strength curves are presented for all load cases in Figures 3-7, and show both elastic effective width results (r) and plastic effective width results (b_e/b), derived from both unwelded and welded plate tests. The residual stress pattern induced in the welded specimens consisted of tension blocks at yield along both longitudinal edges, and a region of approximately constant compressive stress elsewhere, approximating that existing in flame-cut plate elements. The average compressive stress for all welded specimens was 104MPa. Further details of the process and the magnitude of residual stresses induced are given in Bambach and Rasmussen (2001). All curves are plotted with respect to the non-dimensionalised slenderness ratio (Equation 1), where the critical buckling stress (f_{cr}) is calculated by Equation 2.

The buckling coefficient (k) used in Equation 2 is calculated for each strain gradient from the Finite Strip program THINWALL (Papangelis and Hancock 1995), using the asymptotic value found with large half-wavelengths. This is the theoretical solution for a plate simply supported on three sides with the remaining longitudinal edge free. It is noted that the buckling coefficients given in Appendix F of AS/NZS4600 (1996) (the same as those in Table 4.2 of Eurocode 3, Part 1.3 1996), are approximately the same as these. Comparisons of the elastic buckling stress results obtained from the tests with theoretical solutions show sufficient agreement (within 4%) such that the boundary conditions applied by the test rig may be assumed to be simply supported (Bambach and Rasmussen 2002b). However, due to the inherent scatter in test results for elastic buckling stresses (due to the susceptibility to imperfections), it is more convenient to use the theoretical solution for the plate buckling coefficient (Bambach and Rasmussen 2002b).

For all load cases, strength curves were fitted to the test results using a curve of best fit approach. It was found that power curves give the best overall result for plastic effective widths, when considering that the curve must give a good approximation of the test data, whilst maintaining a convenient form for structural design. With these two considerations in mind, the coefficients of the power curves were adjusted until reasonable agreement with the test results was achieved. A similar procedure was applied to the elastic effective width results, where the coefficients of the Winter formula (Equation 7) were adjusted until reasonable agreement with the test results was achieved. Particular emphasis when deriving elastic effective width equations was given to maintaining a form congruent with that currently used in international design

standards. The equations for the strength curves derived from plate test results for the four strain gradients tested are presented in Table 1.

Pure Compression

The elastic and plastic effective width reduction factors (denoted by r and b_e/b respectively) derived from the plate tests for pure compression have the same magnitude, since the effective width is assumed to be at the yield stress for both cases, and the effective widths and are adjacent to the supported edge. The plastic effective width equation for this load case given in Table 1, may be rearranged to Equation 6 for comparison with the Winter (1947) equation for stiffened elements (Equation 7) and the Winter (1970) equation for unstiffened elements (Equation 8), which is the equation for stiffened elements modified such that it better represents the stub column and beam data of Kalyanaraman et al. (1977). The three equations are plotted together in Figure 3 for comparison, as are the authors plate test results and those by Kalyanaraman et al. (1977) on cold-formed sections. The plastic equation proposed by the authors converges with the Winter unstiffened equation at large slenderness values, while sitting slightly below at smaller slenderness values, particularly at slenderness values around 1.5, where both the authors' test results and those by Kalyanaraman are over-predicted by the Winter curve for unstiffened elements.

$$\frac{b_e}{b} = 0.8\left(\sqrt{\frac{f_{ol}}{f_y}}\right)^{\frac{3}{4}} \tag{6}$$

$$\frac{b_e}{b} = \sqrt{\frac{f_{ol}}{f_y}}\left(1 - 0.22\sqrt{\frac{f_{ol}}{f_y}}\right) \tag{7}$$

$$\frac{b_e}{b} = 1.19\sqrt{\frac{f_{ol}}{f_y}}\left(1 - 0.298\sqrt{\frac{f_{ol}}{f_y}}\right) \tag{8}$$

Compressive strain at the free edge, zero at the supported edge

In Figure 4 it is shown that a reduced plastic effective width equation is required compared with the case of pure compression, however the elastic effective width results are in reasonable agreement with the Winter equation (7). The eccentricity of the plastic effective width from the supported edge ($ecc1$) and from the unsupported edge ($ecc2$) (Figure 5) are given by Equations 9-11.

For $l \le 0.654$:

$$\frac{ecc1}{b} = 1 - \frac{b_e}{b} \tag{9}$$

For $l > 0.654$:

$$\frac{ecc1}{b} = 0.45 \tag{10}$$

$$\frac{ecc2}{b} = 0.55 - \frac{b_e}{b} \qquad \ge 0 \tag{11}$$

Compressive strain at the supported edge, zero at the unsupported edge

In Figure 6 it is shown that a reduced plastic effective width equation is required compared with the case of pure compression, however the elastic effective width results are in reasonable agreement with the Winter equation (7). The eccentricity of the plastic effective width from the supported edge was found to be negligible and has been assumed to be zero.

Pure Bending with compression at the unsupported edge

The ultimate condition when deriving plastic effective widths for this load case is taken as the point at which the bending stress is a maximum. Due to limitations of the strokes of the actuators, the ultimate

condition could not be reached in the tests. Analysis using the FEM program Abaqus is compared with the test results for the range tested, and used to determine the ultimate moment. The Abaqus model incorporates the measured material properties and imperfections. Further details are presented in Bambach and Rasmussen (2002b). The Abaqus results for this load case are shown in Figure 7, the plastic effective width factor for the *compressed portion* of the unstiffened element is found to be approximately zero for all slenderness ratios analysed. This is due to the fact that the net force on the section at ultimate is in tension, and is at a magnitude slightly greater than the force created by assuming half the width of the element is at yield in tension. The results for the effective widths are slightly negative, since the assumed stress state is elastic perfectly-plastic, whereas in reality strain hardening occurs in the tension zone. It is noted that at the ultimate condition for plastic effective widths for this load case, being the point at which the moment is a maximum, the strain on the element is as high as 40 times the yield strain, a condition not commonly found in sections. The assumption that this is the ultimate condition then, produces a conservative result for plastic effective widths for this load case. It is also noted that there is no limit applied to this load case for the slenderness ratio beneath which the element will be fully effective. The reason that even the least slender element analysed (slenderness ratio 0.7) is fully ineffective in the compressed portion at ultimate is due to imperfections. While the theoretical buckling stress is approximately 600MPa, lateral displacements are triggered earlier due to the presence of imperfections, and the nature of the applied strain gradient (compression at the unsupported edge and tension at the supported edge) is such that lateral displacements develop rapidly, as observed in the tests. Theoretically there exists a slenderness ratio where the element is so stocky that even with imperfections negligible lateral displacements occur and the element is fully effective. However, the assumption that for all slenderness ratios for this load case the compressed portion of the element is ineffective, simplifies the design equations somewhat for plastic effective widths of elements with maximum compressive strain at the unsupported edge and produces a slightly conservative solution.

The ultimate condition when deriving elastic effective widths for this load case is taken as the point at which first yield occurs in the element. Since the tension zone remains fully effective, this corresponds to the point at which the strain at the supported edge reaches the yield strain. It is noted that the elastic effective width equation that corresponds to the test data approaches 0.5 as the slenderness approaches the practical limit of 3.5 (Figure 7), such that for slender elements the compressed portion is ineffective.

Pure Bending with tension at the unsupported edge

There are no test results for this load case, due to the fact that preliminary investigations revealed that the buckling coefficient for this load case is very high (23.8). As a result, very large b/t ratios in Equation 2 are required in order to obtain elastic buckling stresses. The current limit on b/t ratios for unstiffened elements in AS/NZS4600 (1996) is 60, and from Equation 1 this produces a slenderness ratio of 0.5 (assuming a yield stress of 300MPa). Slenderness ratios of 0.75 (b/t ratio 95), 1.0 (b/t ratio 130), and 1.275 (b/t ratio 155) were analysed with Abaqus and found to be fully effective plastically at ultimate, as one might expect, since the strain gradient of compression at the supported edge and tension at the unsupported edge is very stable and does not encourage the development of lateral displacements. Theoretically there exists a slenderness ratio where the element is so slender that lateral displacements occur in the compressed zone and a portion then becomes ineffective, however this occurs at a b/t ratio beyond practical limits, and we can assume then that practical unstiffened elements under this strain gradient are fully effective plastically (and are correspondingly fully effective elastically also).

This result may be further verified if one considers the compressed portion of the unstiffened element to be similar to a stiffened element under a strain gradient varying from yield to zero strain. In AS/NZS4600 (1996), the element has a buckling coefficient (k) of 8 and is fully effective when the slenderness ratio is less than 0.673, yielding a b/t ratio from Equation 2 of 46.7 (assuming a yield stress of 300MPa). Thus the

unstiffened element under bending is fully effective up to a *b/t* ratio of (2 x 46.7) = 93.4, which is beyond the limit (60) specified for unstiffened elements in AS/NZS4600 (1996). Again we have the result that for all practical unstiffened elements under this load case, the element is fully effective.

DESIGN METHODS FOR EFFECTIVE WIDTHS OF UNSTIFFENED ELEMENTS

The plate test results for effective widths of unstiffened elements under strain gradients are plotted in Figures 8,9 for plastic effective widths and Figures 10,11 for elastic effective widths. The equations presented in Table 1 for tested edge strain ratios (y) of 0, 1 and -1 are shown as solid curves in Figures 8-11. The dashed lines in Figures 8-11 are the results for intermediate edge strain ratios, derived as linear approximations between the edge strain ratios tested.

The equations for intermediate edge strain ratios are presented as a general design method for *plastic* effective widths in Table 2, in a similar format to Appendix F of AS/NZS4600 (1996) and Table 4.2 of Eurocode 3, Part 1.3 (1996). In Table 2 the equations for the buckling coefficient (k) are unchanged, however the proposed plastic effective width equations have been inserted in lieu of those in AS/NZS4600 and Eurocode 3. It is noted that Appendix F of AS/NZS 4600 refers to (y) as the ratio of the edge stresses calculated on the basis of the full section, and is thus congruent with the ratio of edge strains described in this report.

The equations for intermediate edge strain ratios are presented as a general design method for *elastic* effective widths by Equations 12-15. The advantage of this model is that the effective width factor (r) multiplied by the gross element width (b) gives the effective width of the element measured from the supported edge, which is congruent with current standards. The edge strain ratio (y) is expressed as the ratio of the edge stresses calculated on the basis of the full section in order to be consistent with current international standards.

Where the stress increases toward the unstiffened edge of the element:

$$\text{For } y \geq 0 \qquad r = \frac{\left(1 - \frac{0.22}{l}\right)}{l} \qquad r \leq 1 \tag{12}$$

$$\text{For } y < 0 \qquad r = (1 - y)\frac{\left(1 - \frac{0.22(1-y)}{l}\right)}{l} \qquad r \leq 1 \tag{13}$$

Where the stress decreases toward the unstiffened edge of the element:

$$\text{For } y \geq 0 \qquad r = \frac{\left(1 - \frac{0.22}{l}\right)}{l} \qquad r \leq 1 \tag{14}$$

$$\text{For } y < 0 \qquad r = (1 + y)\frac{\left(1 - \frac{0.22}{l}\right)}{l} - y \qquad r \leq 1 \tag{15}$$

$y = \frac{f_2^*}{f_1^*}$ where f_1^*, f_2^* = edge stresses calculated on the basis of the full section

CONCLUSIONS

Plate test results for unstiffened elements under a variety of strain gradients are presented in the form of strength curves, and equations for predicting the effective widths are derived. It is shown that the difference between welded and unwelded plate test results is small, such that the same effective width equations may be applied to both cases. This conclusion applies to a residual stress pattern with tension at both longitudinal edges and approximately constant compression elsewhere, as is found in flame-cut plate elements.

It is shown that plastic effective widths at an eccentricity from the supported edge may be derived from the plate test results, and represent exactly both the ultimate force and moment in the plate tests. Elastic effective widths adjacent to the supported edge may also be derived from the plate test results, satisfying the ultimate force but underestimating the ultimate moment in the plate tests. Both elastic and plastic effective widths are derived from the plate test results, and general design equations for predicting elastic and plastic effective widths of unstiffened elements under stress gradients are presented.

In a companion report (Bambach and Rasmussen 2002a), the plastic effective width equations obtained herein are used to produce a general design procedure for sections that contain unstiffened elements under stress gradients, beyond the point of initiation of yielding in the section, and are shown to compare well with section test data of I-sections and channel sections in minor axis bending. While the elastic effective width equations obtained herein do not match exactly both the ultimate force and moment values of the plate tests from which they were derived, it is shown in the companion report that good agreement with section test data may also be achieved with elastic effective widths, when inelastic reserve capacity is taken into account.

REFERENCES

AISI (1996). *Specification for the Design of Cold-Formed Steel Structural Members*. American Iron and Steel Institute, Washington D.C.

AS/NZS 4100 (1998). *Australian/New Zealand Standard. Steel Structures*. Standards Australia, Sydney.

AS/NZS 4600 (1996). *Australian/New Zealand Standard. Cold-Formed Steel Structures*. Standards Australia, Sydney.

Bambach, M. R. and Rasmussen, K. J. R. (2001). "Residual Stresses in Unstiffened Plate Specimens". *Proc., Third International Conference on Thin-Walled Structures*, Zaras, J., Kowal-Michalska, K. and Rhodes, J., eds., Elsevier, Cracow, Poland, 87-93.

Bambach, M. R. and Rasmussen, K. J. R. (2002a). "Design models for Thin-Walled Sections in Bending containing Unstiffened Elements." *Research Report, R820*, Department of Civil Engineering, University of Sydney, Sydney.

Bambach, M. R. and Rasmussen, K. J. R. (2002b). "Tests of Unstiffened Plate Elements under combined Compression and Bending." *Research Report, R818*, Department of Civil Engineering, University of Sydney, Sydney.

Beale, R. G., Godley, M. H. R. and Enjily, V. (2001). "A Theoretical and Experimental Investigation into Cold-formed channel sections in Bending with the Unstiffened Flanges in Compression." *Computers and Structures*, 79, 2403-2411.

Chick, C. G. (1997). *Thin-Walled I-Sections in Compression and Bending*. PhD Thesis, Sydney University, Sydney.

Chick, C. G. and Rasmussen, K. J. R. (1999). "Thin-Walled Beam-Columns. 2:Proportional Loading Tests." *Journal of Structural Engineering, ASCE*, 125(11), 1267-1276.

Desmond, T. P., Pekoz, T. and Winter, G. (1981). "Edge Stiffeners for Thin-Walled Members." *Journal of the Structural Division, ASCE*, 107(ST2), 329-353.

Eurocode 3 (1992). *Eurocode 3: Design of Steel Structures, Part 1.1: General Rules and Rules for Buildings*. European Committee for Standardisation, European Prestandard, ENV 1993-1-3, Brussels.

Eurocode 3 (1996). *Eurocode 3: Design of Steel Structures, Part 1.3: General Rules - Supplementary Rules for Cold Formed Thin Gauge Members and Sheeting*. European Committee for Standardisation, European Prestandard, ENV 1993-1-3, Brussels.

Kalyanaraman, V., Pekoz, T. and Winter, G. (1977). "Unstiffened Compression Elements." *Journal of the Structural Division, ASCE*, 103(ST9), 1833-1848.

Papangelis, J. P. and Hancock, G. J. (1995). "Computer Analysis of Thin-Walled Structural Members." *Computers and Structures*, 56(1).

Rhodes, J. (2000). "Buckling of Thin Plates and Thin-Plate Members". *Proc., Structural Failure and Plasticity, IMPLAST 2000*, Zhao, X. L. and Grzebieta, R. H., eds., Elselvier, 21-42.

Rhodes, J., Harvey, J. M. and Fok, W. C. (1975). "The Load-Carrying Capacity of Initially Imperfect Eccentrically Loaded Plates." *International Journal of Mechanical Sciences*, 17, 161-175.

Rusch, A. and Lindner, J. (2001). "Remarks to the Direct Strength Method." *Thin-Walled Structures*, 39, 807-820.

Winter, G. (1947). "Strength of Thin Steel Compression Flanges." *Transactions, ASCE*, 112, 527-576.

Winter, G. (1970). *Commentary on the 1968 Edition of the Specification for the Design of Cold-Formed Steel Structural Members*. American Iron and Steel Institute, New York.

Yiu, F. and Pekoz, T. (2001). "Design of Cold-Formed Steel Plain Channels. Final Report." Cornell University, Ithaca, USA.

Strain gradient in plate test	Elastic effective width adjacent to the supported edge Effective width= $\rho.b$	Plastic effective width at an eccentricity to the supported edge Effective width of the compressed portion=b_e	Strength curve
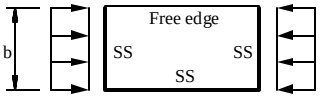	$\rho = \frac{\left(1-\frac{0.22}{\lambda}\right)}{\lambda}$ 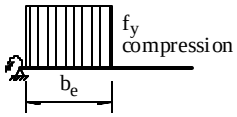	$\frac{b_e}{b} = 0.8\lambda^{-\frac{3}{4}}$ 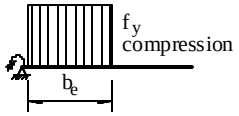	**Figure 3**
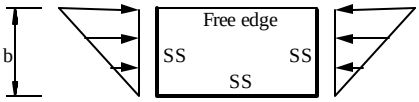	$\rho = \frac{\left(1-\frac{0.22}{\lambda}\right)}{\lambda}$ 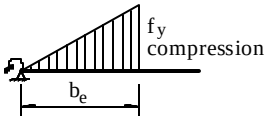	$\frac{b_e}{b} = 0.4\lambda^{-\frac{3}{4}}$ Eccentricity equations 9-11 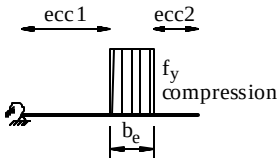	**Figure 4**
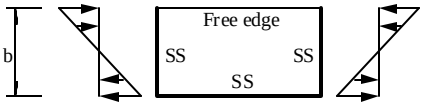	$\rho = \frac{2\left(1-\frac{0.44}{\lambda}\right)}{\lambda}$ 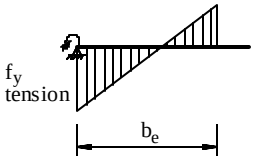	$\frac{b_e}{b} = 0$ 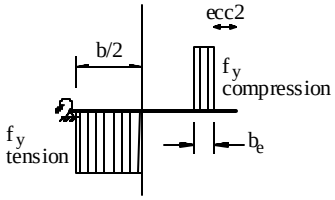	**Figure 7**
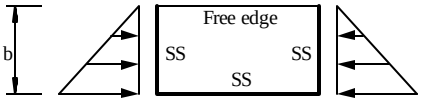	$\rho = \frac{\left(1-\frac{0.22}{\lambda}\right)}{\lambda}$ 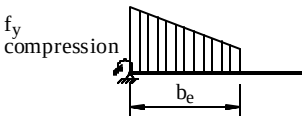	$\frac{b_e}{b} = 0.6\lambda^{-\frac{3}{4}}$ 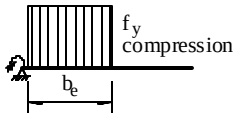	**Figure 6**

Table 1 : Elastic and plastic effective width equations derived from plate tests

PLATE BUCKLING COEFFICIENTS (k) AND EFFECTIVE WIDTHS (b_e)

Stress distribution (compressive positive)	Effective width (b_e)
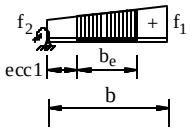	For $1 > \psi \geq 0$: $\frac{b_e}{b} = 0.4(1+y)\,l^{-\frac{3}{4}} \leq 1$ $\frac{ecc1}{b} = 0.45(1-y) \leq 1-\frac{b_e}{b}$
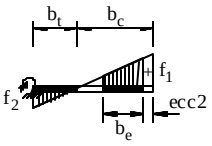	For $\psi < 0$: $\frac{b_e}{b} = 0.4(1+y)\,l^{-\frac{3}{4}} \leq \frac{b_c}{b}$ $\frac{ecc2}{b} = 0.55(1+y) - \frac{b_e}{b}$

$\psi = f_2^*/f_1^*$	+1	0	−1	$+1 \geq \psi \geq -1$
Plate buckling coefficient (k)	0.43	0.57	0.85	$0.57 - 0.21\psi + 0.07\psi^2$

Stress distribution (compressive positive)	Effective width (b_e)
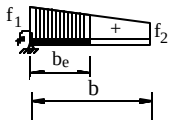	For $1 > \psi \geq 0$: $\frac{b_e}{b} = 0.2(3+y)\,l^{-\frac{3}{4}} \leq 1$
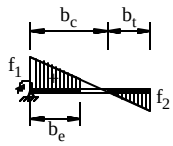	For $\psi < 0$: $\frac{b_e}{b} = 0.6(1+y)\,l^{-\frac{3}{4}} - 0.5y \leq \frac{b_c}{b}$

$\psi = f_2^*/f_1^*$	+1	$1 > \psi > 0$	0	$0 > \psi > -1$	−1
Plate buckling coefficient (k)	0.43	$\frac{0.578}{\psi + 0.34}$	1.70	$1.70 - 5\psi + 17.1\psi^2$	23.8

NOTE: f_1^* and f_2^* are web stresses calculated on the basis of the full section.

Table 2: Plastic effective width method for unstiffened elements under stress gradients

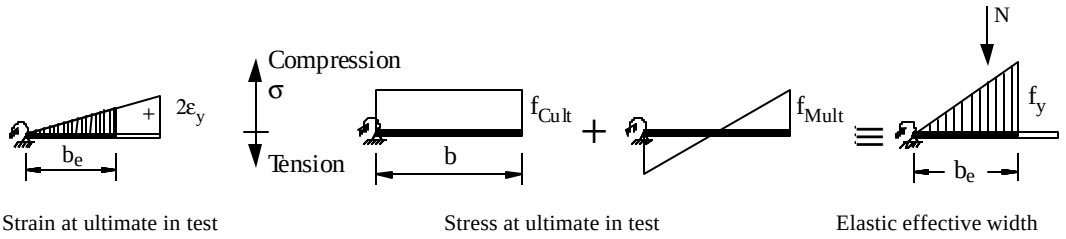

Figure 1 : Deriving elastic effective widths from plate tests of compressive strain at the unsupported edge, zero at the supported edge

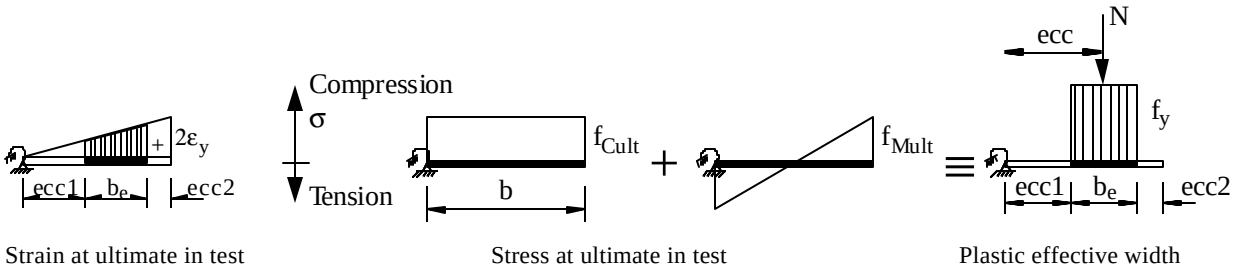

Figure 2: Deriving plastic effective widths from plate tests of compressive strain at the unsupported edge, zero at the supported edge

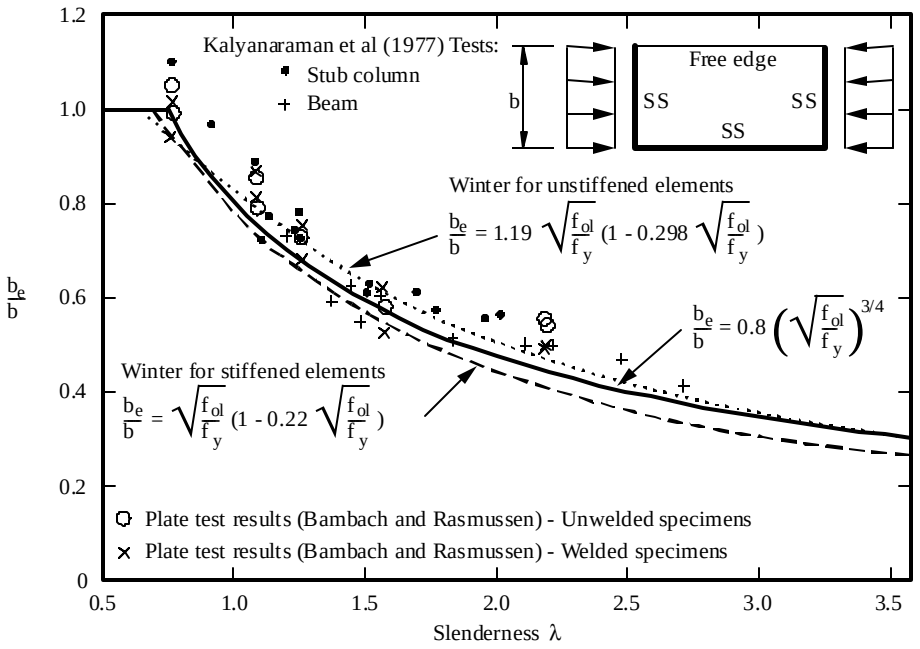

Figure 3: Strength curve for pure compression plate tests compared with Winter formulae and section tests of Kalyanaraman et al (1977), *k*=0.43

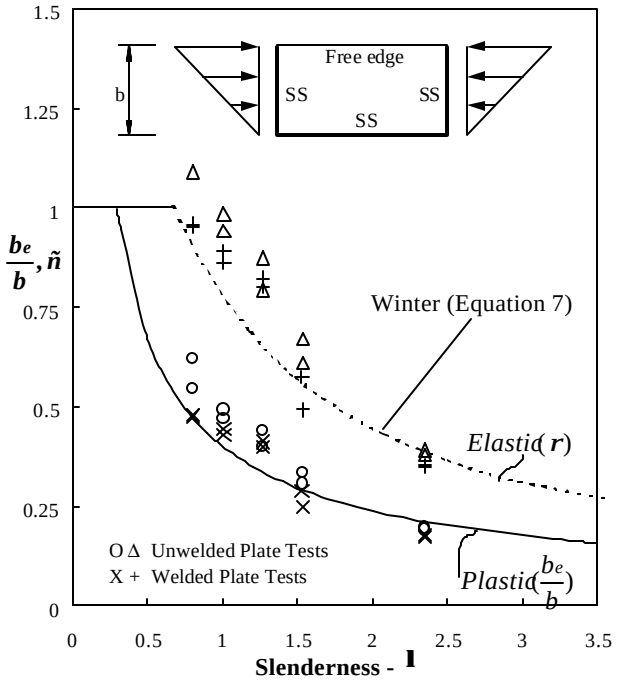

Figure 4: Strength curve- compressive strain at the unsupported edge, zero at the supported edge, *k*=0.57

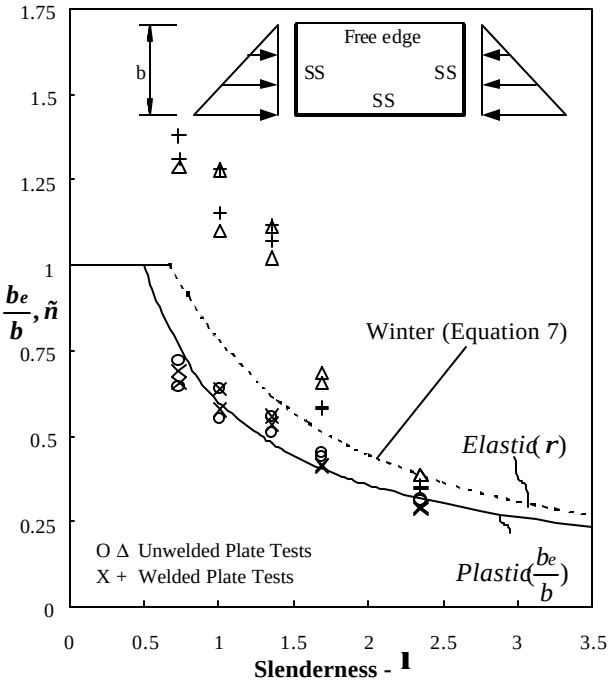

Figure 6: Strength curve – compressive strain at the supported edge, zero at the unsupported edge, *k*=1.70

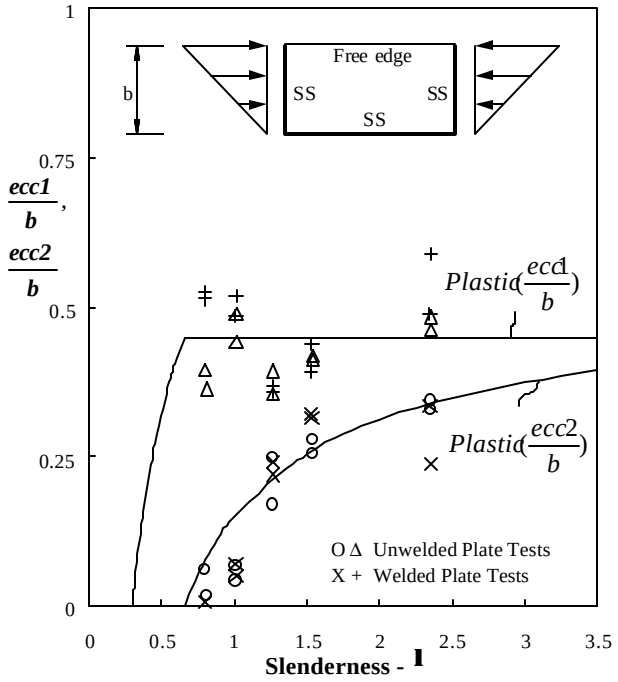

Figure 5: Strength curve- compressive strain at the unsupported edge, zero at the supported edge, *k*=0.57

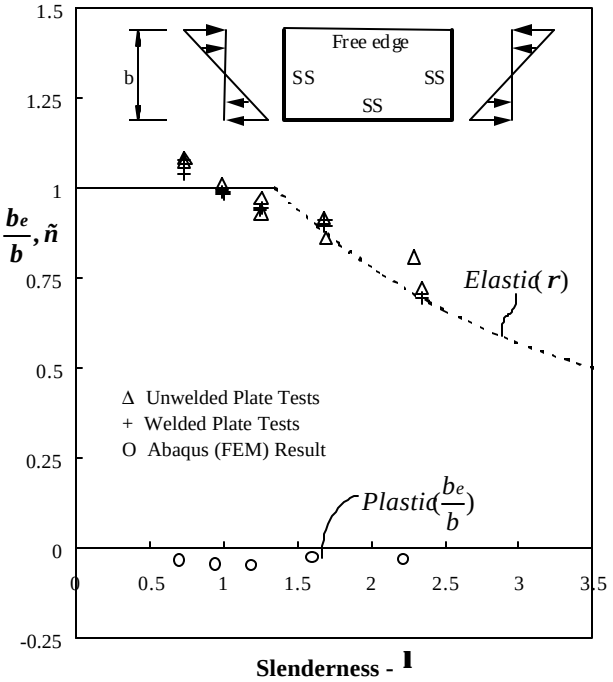

Figure 7: Strength curve– pure bending, *k*=0.85

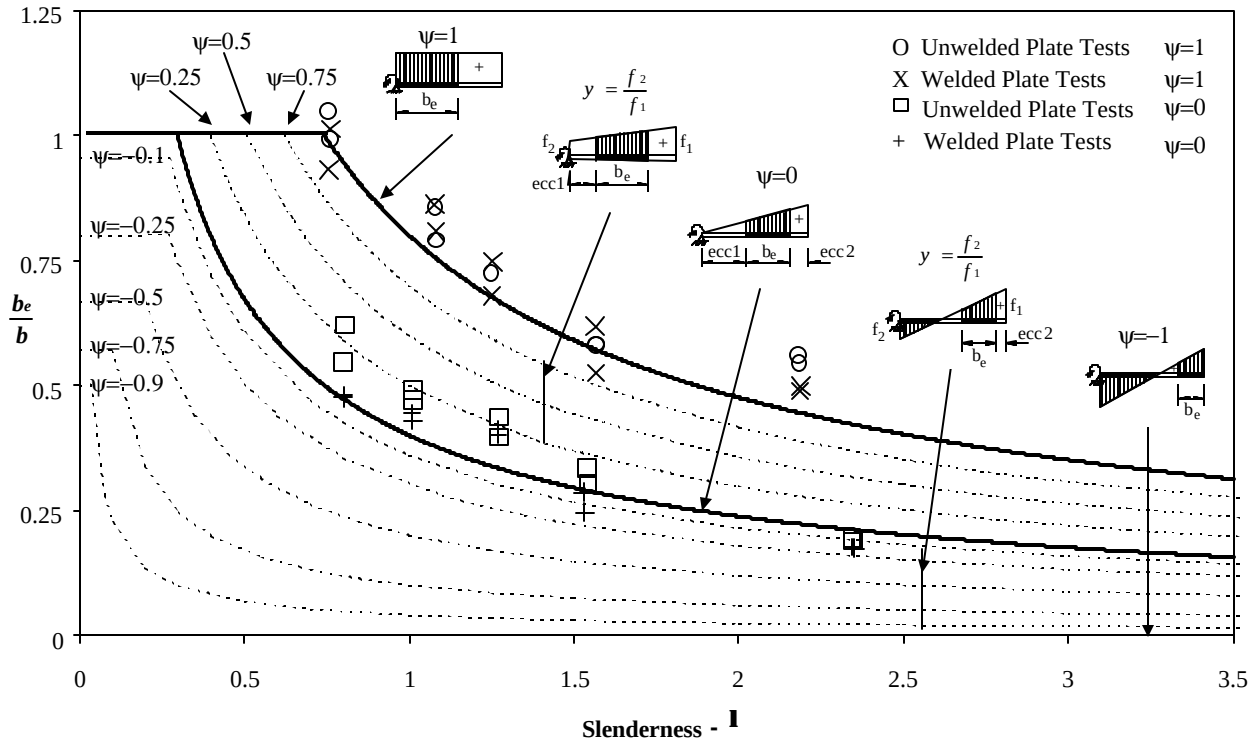

Figure 8: Plastic effective widths – strain gradients with maximum compressive strain at the unsupported edge

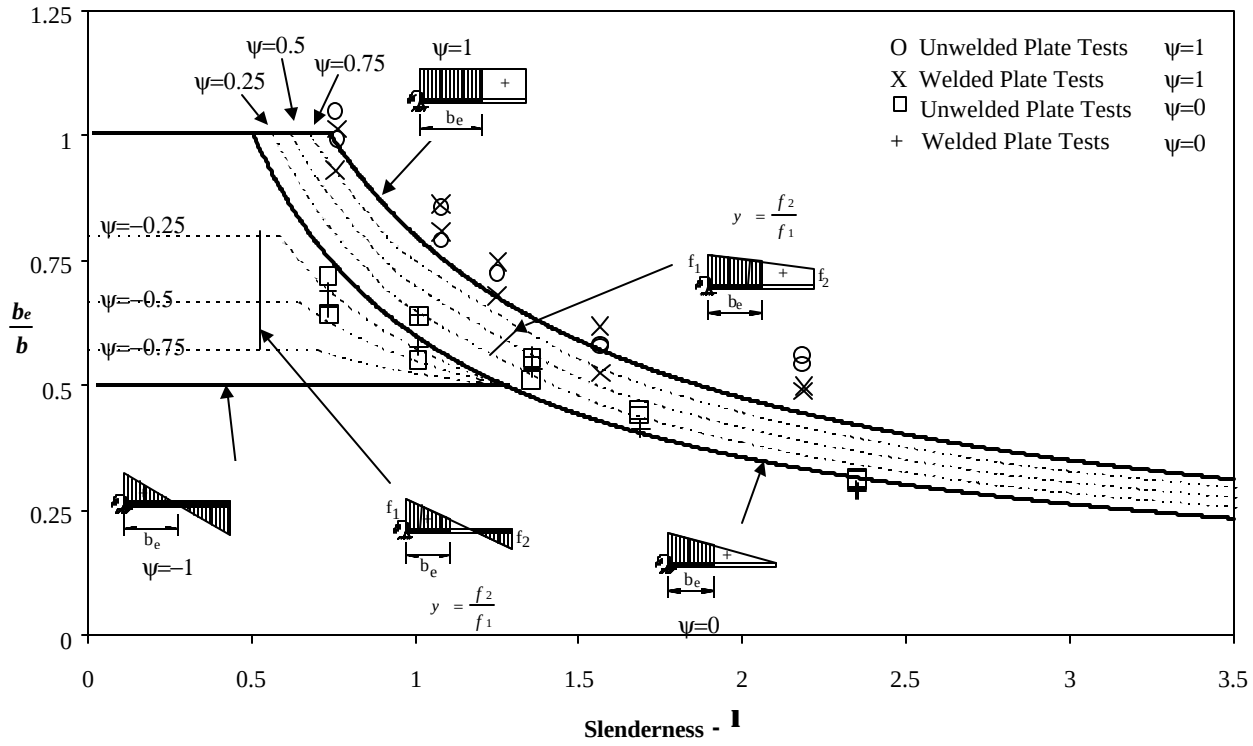

Figure 9: Plastic effective widths - strain gradients with maximum compressive strain at the supported edge

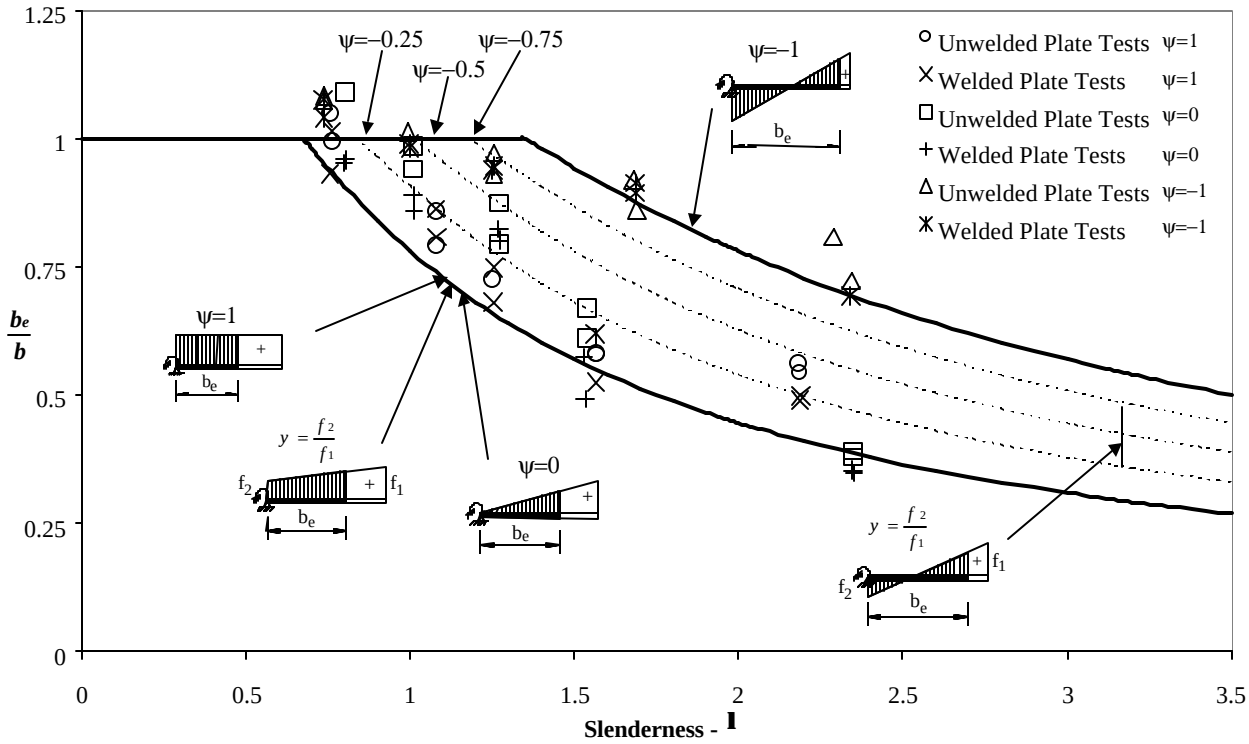

Figure 10: Elastic effective widths - strain gradients with maximum compressive strain at the unsupported edge

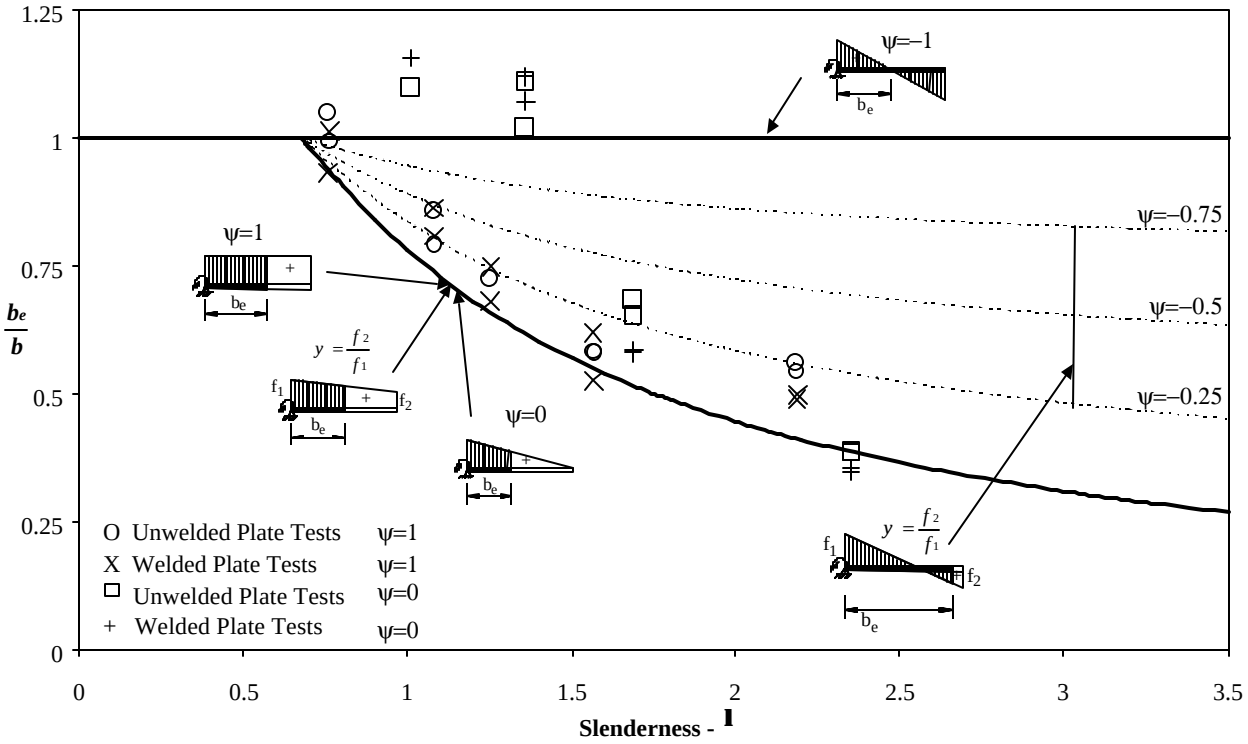

Figure 11: Elastic effective widths - strain gradients with maximum compressive strain at the supported edge